

# Synthesis and characterization of gum acacia stabilized zinc oxide / titanium dioxide nanoparticles embedded with Entacapone for in vitro drug release

Seema FIRDOUSE\*<sup>1</sup>, Umme HABEEBA<sup>1</sup>, Parwez ALAM<sup>2</sup>, Chaitanya MITTA<sup>3</sup>, SwatiKALEPU<sup>3</sup>, Shoyeb AHMED<sup>1</sup>

<sup>1</sup> Department of Pharmaceutical Analysis, Anwarul Uloom College of Pharmacy, Hyderabad, Telangana-500001, India

<sup>2</sup> Department of Pharmacognosy, Shadan College of Pharmacy, Peerancheru, Hyderabad, Telangana-500091, India

<sup>3</sup> Department of Pharmaceutical Analysis, Bojjam Narasimhulu Pharmacy College for Women, Hyderabad, Telangana 500059, India.

\*Corresponding Author. E-mail: [seemamiyna@gmail.com](mailto:seemamiyna@gmail.com) (S.F.); Tel. +918790741514.

Received: 6 June 2023 / Revised: 3 January 2024 / Accepted: 4 January 2024

**ABSTRACT:** Nanotechnology is among the most developing aspects of the medical stream. Gum acacia (GA), being biocompatible, naturally occurring, non-toxic, and inexpensive polymer, has gained tremendous attention in the field of pharmacy. The nanoparticle production using Gum acacia as a template led to more stable drug delivery systems. Zinc oxide (ZnO) and Titanium dioxide (TiO<sub>2</sub>) possess potential biological applications including anticancer activity, antimicrobial activity, bioimaging, and potent drug carrier properties. The synthesis of Gum acacia stabilized Zinc oxide and Titanium dioxide nanoparticles incorporated with Entacapone an antiparkinsonian drug, was carried out keeping in view all these aspects. Entacapone is a combination of drug therapy with levodopa and carbidopa in the treatment of Parkinson's disease (a neuro-degenerative disorder). The synthesized drug - nanocomposite showed extended release or sustained-release properties. According to the experimental results, it is reported that the Gum acacia along with ZnO and TiO<sub>2</sub> acts as a drug delivery carrier releasing Entacapone at the intended site in desired time and quantity.

**KEYWORDS:** Nanoparticles; Drug delivery carrier; Sustained release; Entacapone; Anti-parkinsonian drug.

## 1. INTRODUCTION

Nanotechnology encompasses the intricate process of manufacturing or synthesizing materials at the nano-scale, a realm where particles have sizes that are typically in the range of 1-100 nanometers. possessing novel functionalities and improved characteristics[1]. Nanotechnology is an emerging field that holds great promise for various industries and sectors. With the ability to manipulate materials and particles at the nanoscale level, nanotechnology has opened up new possibilities for the development of novel treatments and solutions that can significantly impact public health[2]. By harnessing the unique properties and behaviors of materials at the nanoscale, researchers have been able to create new tools and materials that have revolutionized industries such as engineering, electronics, and medicine. The impact of nanotechnology on the global economy cannot be understated[3]. Nanostructured materials have played a crucial role in improving the quality of life for individuals around the world. greater success in numerous applications including, medicine, health care, physics, optics, energy, catalysis, water, environment, and electronics[4]. They are important ingredients in ceramics, paints, metals, plastics, and magnetic materials [5]. There has been a tremendous increase in nanotechnology in the past decades due to its applications in medicine, chemistry, and biotechnology[6]. The utilization of nanoparticles has garnered significant interest due to their beneficial effects in various sectors, such as consumer products, pharmaceuticals, cosmetics, transportation, energy, and agriculture. These NPs are currently being produced for a multitude of novel applications within the industry [7].

Nanoparticles are minute hollow structures, and with their significantly smaller dimensions, they cannot be detected through conventional microscopes and instead require the use of an electron microscope for observation. These particles exhibit various forms including spheres, tubes, colloids, quantum dots, fibers, rods, crystals, fullerenes, etc., and can contain a range of materials such as oxides, metals, salts, polymers,

**How to cite this article:** Firdouse S, HabeebaU, Alam P, Chaitanya M, Swati K, Ahmed S. Synthesis and characterization of gum acacia stabilized zinc oxide / titanium dioxide nanoparticles embedded with entacapone for in vitro drug release. J Res Pharm. 2025; 29(1): 384-395.

and aerosols. For a full description, it is necessary to measure their additional physical characteristics, such as size, shape, surface characteristics, crystallinity, and dispersion state[5,6].

To produce the best possible biological results, nanoparticles are being researched as prospective medication delivery systems. To achieve targeted delivery or extended-release, different medications, biomolecules, or growth factors can be combined with nanoparticles. The controlled delivery of the loaded drugs is made possible by nanoparticle-assisted drug delivery to produce the desired biological effects. In nutritional supplements, the nanoparticles are also employed to deliver physiologically active ingredients, such as minerals. The cavities are used to capture signaling molecules for precise targeting in analytical applications[5,7].

The dried sticky exudate of Acacia Senegal and other Acacia species that are members of the Leguminosae family is known as gum acacia (GA). GA includes the Arabic acid salts of magnesium, calcium, and potassium. In the primary galactosyl chain of GA, D-galactose, L-rhamnose, L-arabinose, and D-glucuronic acid are all present. By -D-(13) connections, these galactosyl units are connected. Using -D-(16) connections, the side chain is connected to the main chain[8]. It serves as a binder, emulsifier, thickening agent, glue, and other things. Just two of the many bacterial species that zinc oxide (ZnO) demonstrates antibacterial activity against are gram-negative and gram-positive bacteria.

The synthesis of ZnO nanocomposites can be carried out by using various methods such as evaporation, pulse laser deposition, sol-gel method, etc[9]. The ZnO nanoparticles manufactured in the absence of GA showed less antibacterial activity when compared to GA-ZnO nanoparticles. This can be related to the decrease in the average size of the particles when GA is used to stabilize the ZnO nanoparticles[10]. Titanium dioxide (TiO<sub>2</sub>) is used as a pigment in food products, cosmetics, nano research, etc. The clinical analysis indicates that the TiO<sub>2</sub> nanoparticles enter the systemic circulation and cross various cell membranes including blood placenta and blood-brain barriers after ingestion[11]. TiO<sub>2</sub> NPs can be manufactured by using various processes including metal-organic chemical vapor deposition, reverse micelles gas phase synthesis, and wet chemical synthesis[12].

Current research work aims to synthesize Gum acacia stabilized Zinc oxide (ZnO) / Titanium dioxide (TiO<sub>2</sub>) nanoparticles embedded with Entacapone, an antiparkinsonian drug to achieve extended release or sustained release drug substance in the form of nanoparticles, for its invitro drug release.

The synthesized drug nanocomposite was analyzed by various characterization techniques including X-ray diffraction (XRD), Scanning electron microscopy (SEM), Ultraviolet-visible - Diffuse reflectance spectrum (UV-DRS), Differential scanning calorimetry (DSC), Thermogravimetric analysis (TGA), Derivative thermal gravimetry (DTG), Fourier transform infrared spectroscopy (FTIR) and Mass spectroscopy (MS). The percentage drug release data of the nanocomposite was also established using in vitro drug release studies by UV-visible absorption spectra.

## 2.RESULTS AND DISCUSSION

### 2.1. XRD-Studies

Figure 1a represents the X-ray diffraction pattern of the Gum acacia with zinc oxide along with titanium dioxide nanocomposite. The nanocomposite average particle size was found to be 14.72nm, calculated using Scherrer's formula[13]. Figure 1b represents the XRD graph of Gum acacia with Zinc oxide (ZnO) and Titanium dioxide (TiO<sub>2</sub>) loaded with Entacapone drug. The particle size of the nanocomposite along with the drug when taken as average was found to be 9.54nm ±1.25nm. The diffraction peaks located at 23.53°, 30.31°, 38.64°, 47.13°, 54.42°, 61.32° and 65.58° have been depicted as the hexagonal wurtzite phase of GA- ZnO-TiO<sub>2</sub>. other peaks represent the presence of entacapone drug in the nanocomposite loaded inside the composite. The diameter of the synthesized nanocomposite GA-ZnO-TiO<sub>2</sub> loaded with the entacapone drug was calculated using the Debye-Scherrer formula [14].

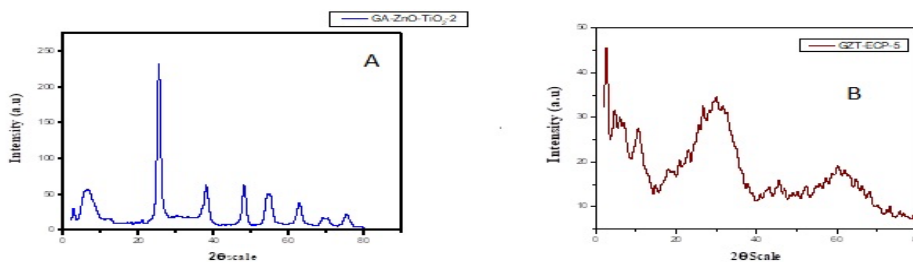


Figure 1. XRD Graph of a) GA-ZnO-TiO<sub>2</sub> b) GA-ZnO-TiO<sub>2</sub>-Entacapone

## 2.2. SEM Analysis [6,7]

The Scanning electron microscope (SEM) images in Figure 2a and 2b provide valuable information about the morphology and structure of Gum acacia with zinc oxide and titanium dioxide at different magnifications. These images depict the approximate helices, zig-zag, nanowires, and round and hollow structures of the nanoparticles. It can also be observed that the mean size of the nanoparticles is 9.603 micrometer and the standard deviation is 1.92 which is in good agreement with the particle sizes calculated from the Debye-Scherrer formula [15,16].

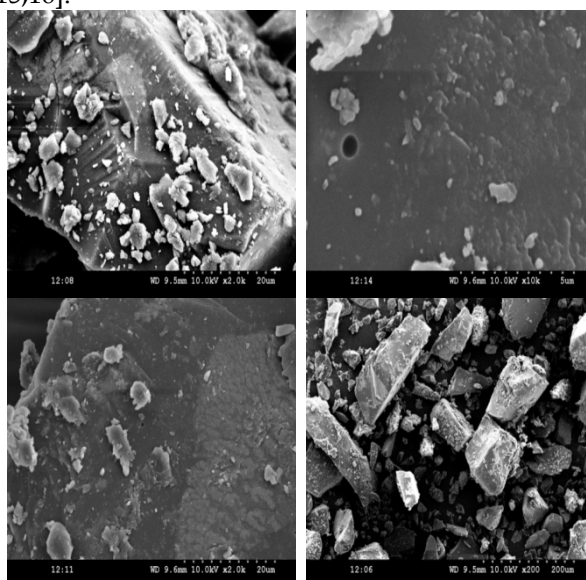


Figure 2a. SEM images of GA-ZnO-TiO<sub>2</sub>

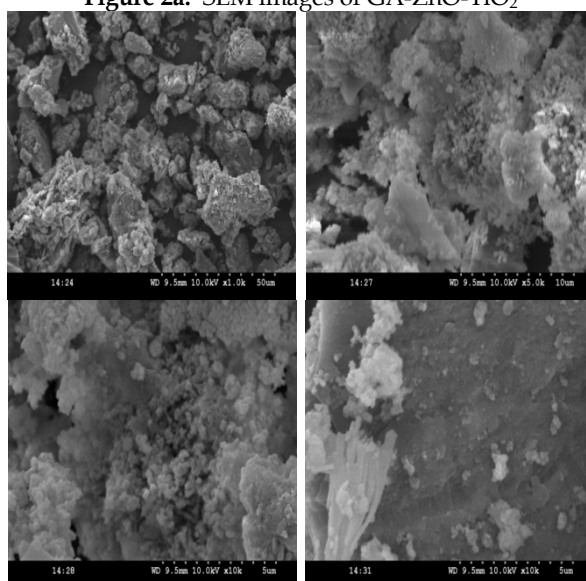


Figure 2b. SEM images of GA-ZnO-TiO<sub>2</sub> loaded with Entacapone

### 2.3. UV-DRS spectroscopic studies

Figure 3a represents the UV-Visible - Diffuse reflectance spectroscopy of Gum acacia along with Zinc oxide and Titanium dioxide[17]. The UV-DRS graph indicates that the sample has a strong absorption maximum below 500nm. Fig.3b represents the UV- Visible - Diffuse reflectance spectroscopy of Entacapone drug alone. Fig.3c represents the UV-Visible diffuse reflectance spectroscopy of Gum acacia along with Zinc oxide and Titanium dioxide loaded with entacapone drug. The absorption maximum of the nanocomposite increases from 250 nm.

The graph shows that the sample have a strong absorption maximum below 500nm. The band gap energy of the composite can be measured by the extrapolation of the linear portion of the graph. UV-Visible diffuse reflectance spectroscopy of Gum acacia along with Zinc oxide and Titanium dioxide loaded with entacapone drug. The absorption maximum of the nanocomposite increases from 250 nm.

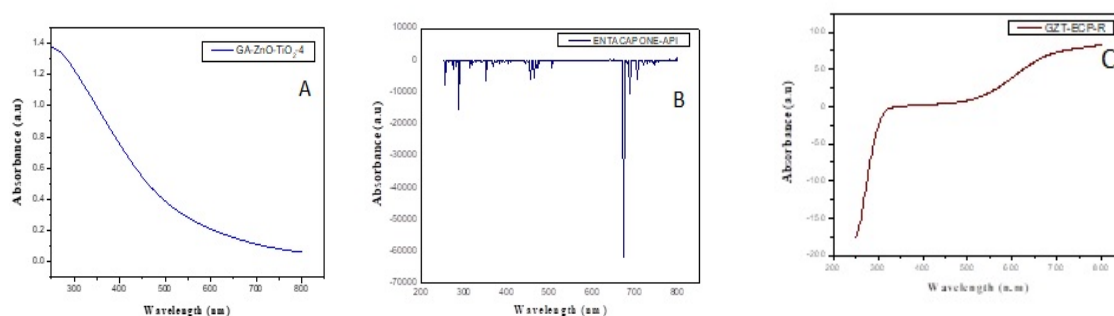


Figure 3. UV-DRS of A) GA-ZnO-TiO<sub>2</sub> B) Entacapone API C) GA-ZnO-TiO<sub>2</sub>-Entacapone

### 2.4. Differential Scanning Calorimetry (DSC)

The thermogram of the Gum acacia sample by differential scanning calorimetry shows the endothermic peak at 310°C. Various exothermic peaks occur at different points as shown in Figure 4A. The DSC graph of Entacapone (Active Pharmaceutical Ingredient) represented in Figure shows the endothermic peak at 164°C. An exothermic peak is also observed at 260°C as shown in Figure 4B. The DSC graph of Gum acacia along with Zinc oxide and Titanium dioxide incorporated with Entacapone represented, shows an endothermic peak at 164°C. An additional endothermic peak is also observed at 70°C. This graph represents the decomposition of the composite at the melting point of the drug i.e. 164°C represents the drug's presence in the composite as shown in Figure 4C, increasing from 250 nm[18].

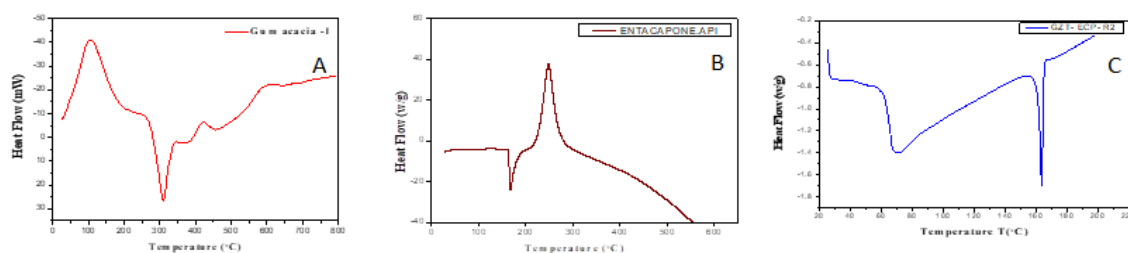


Figure 4. DSC Graph of A) Gum acacia B) Entacapone C)GA-ZnO-TiO<sub>2</sub>-Entacapone

### 2.5. Thermo Gravimetric Analysis (TGA)

The differential thermogravimetric analysis was conducted on Gum Acacia and Entacapone separately, as well as in the composite GA-ZnO-TiO<sub>2</sub>. In the TGA graphs shown in Figure 6A, a peak at approximately 310°C is observed for Gum Acacia, while in Figure 6B, a peak at around 250°C is observed for Entacapone. The DTG graph of GA-ZnO-TiO<sub>2</sub> incorporated with Entacapone as shown in Figure 6C confirms the presence of both components based on their characteristic peaks. The decomposition of Gum

Acacia occurs at around 310°C, as indicated by the peak in its TGA graph as shown in Figure 6A. Moreover, the peak observed at approximately 250°C in the DTG graph of Entacapone as shown in Figure 6B, suggests its decomposition at that temperature. These TGA and DTG curves indicate the thermal stability and degradation behavior of Gum Acacia and Entacapone, both individually and in the composite material. The presence of characteristic peaks at specific temperatures in the TGA and DTG curves indicates the decomposition behavior of Gum Acacia and Entacapone[19,20].

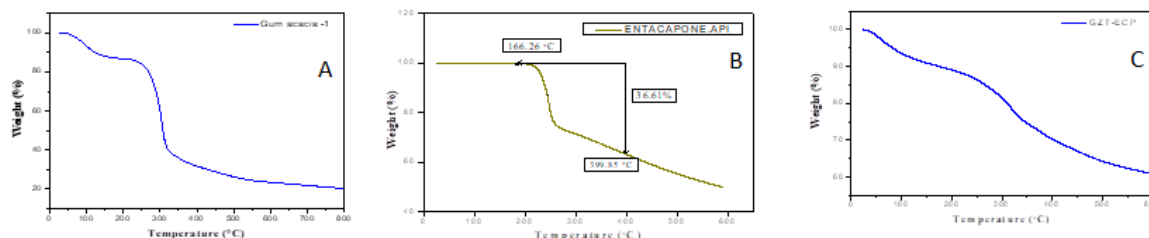


Figure 5. TGA Graph of A) Gum acacia B) Entacapone C) GA-ZnO-TiO<sub>2</sub>-Entacapone

## 2.6. Differential Thermo Gravimetry (TGA)

DTG graph of Gum acacia where the rate of weight change with temperature is seen. The peak is observed at nearly 310°C as shown in Figure 6A. The DTG graph of Entacapone is represented in figure where the derivative weight percentage is plotted against temperature and the peak is observed at around 250°C as shown in Figure 6B. DTG graph of GA - ZnO-TiO<sub>2</sub> incorporated with Entacapone. In this, the rate of weight change is represented by temperature. The peaks characteristic of Gum acacia and Entacapone individually are represented in this graph confirming its presence in the composite as shown in Figure. 6C [21,22].

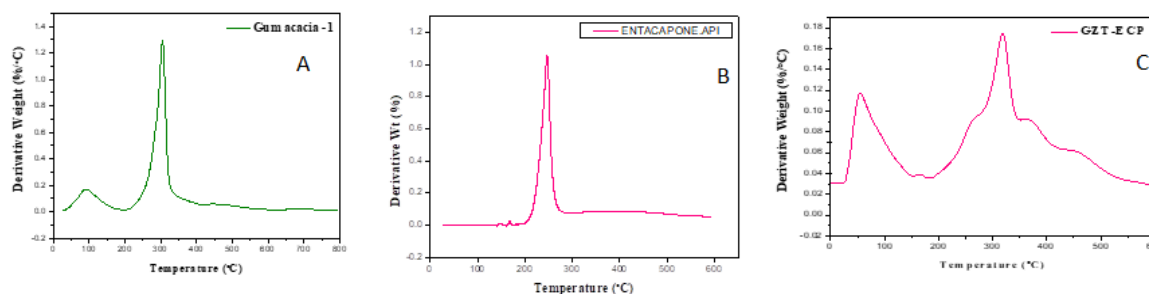


Figure 6. DTG Graph of A) Gum acacia B) Entacapone B) GA-ZnO-TiO<sub>2</sub>-Entacapone

## 2.7. FT-IR Spectroscopic studies

FTIR of the Gum acacia in the range of 4000-500cm<sup>-1</sup>. An intense absorption peak was detected at approximately 3411.84 cm<sup>-1</sup>. Several absorption bands at 2930.85, 2139.23, 1614.72, 1424.51, 1254.79, 1068.18, 772.38, and 614.46 cm<sup>-1</sup> were also observed as shown in Figure 7a. These absorption bands show the purity of the Gum acacia. FTIR pattern of Entacapone drug in the range of 4000-500 cm<sup>-1</sup>. A broad absorption band was observed at 3337.83 cm<sup>-1</sup>. Several absorption bands at 3090.41, 2975.80, 2887.67, 2742.07, 2634.10, 2476.71, 2215.68, 1753.19, 1604.36, 1542.67, 1442.93, 1349.87, 1292.77, 1205.85, 1152.70, 1072.38, 1014.00, 947.32, 873.61, 774.84, 631.25, 562.76, 520.67 and 443.97 cm<sup>-1</sup> were also observed as shown in Figure 7b. These absorption bands are the characteristic of the sample and thus show its purity. FTIR pattern of Gum acacia along with zinc oxide and titanium dioxide loaded with Entacapone in the range of 4000-500 cm<sup>-1</sup>. A broad absorption band was observed at 3340.18 cm<sup>-1</sup>. Several other bands were also observed at 2979.48, 2214.24, 1606.85, 1519.27, 1439.61, 1343.74, 1274.38, 1209.45, 1149.87, 1103.15, 1069.53, 1024.29, 942.86, 874.33, 773.64, 742.67, 629.51 and 521.13 cm<sup>-1</sup> as shown in Figure 7c. These absorption bands show the purity of the composite[23].

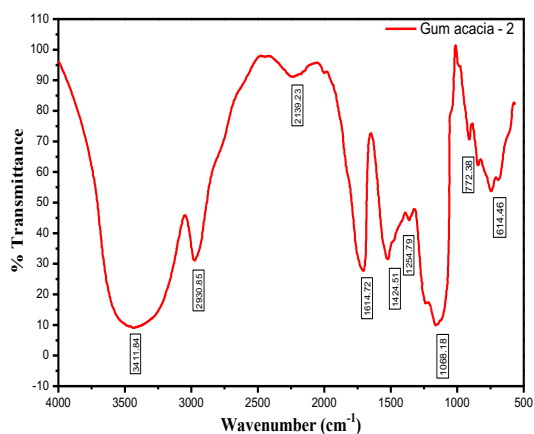


Figure 7a. FTIR of Gum acacia

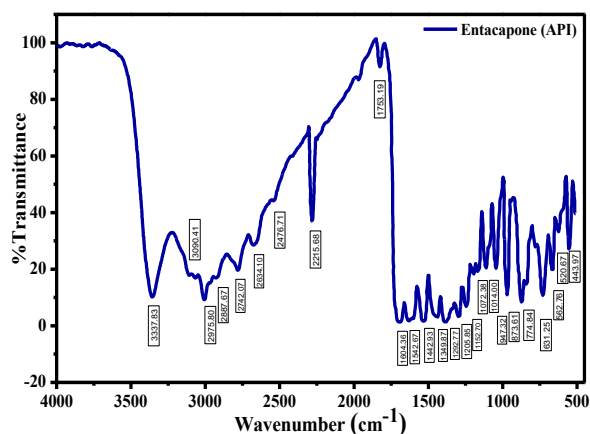


Figure 7b. FTIR of Entacapone

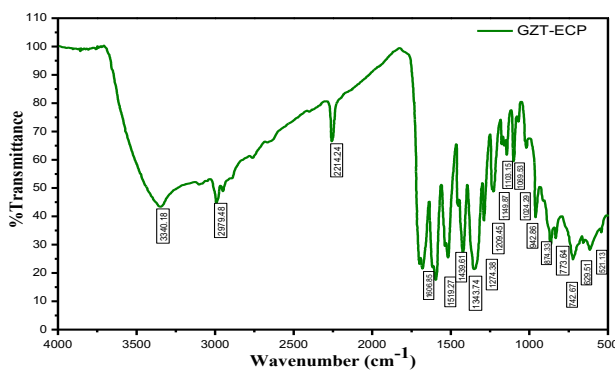


Figure 7c. FTIR of GA-ZnO-TiO<sub>2</sub> loaded with Entacapone

## 2.8. Mass Spectroscopic Studies

Mass spectrum of Gum acacia along with Zinc oxide and Titanium dioxide loaded with Entacapone. The presence of a peak at 15, shows the presence of methyl (CH<sub>3</sub>) group. The peak at 17 shows the hydroxyl (OH) group. At 26, it represents a cyanogen i.e. an acetonitrile group, and at 46, it represents nitrogen dioxide. These molecules make up the broken structure of entacapone. As a result, it depicts the drug's ionization.[24].

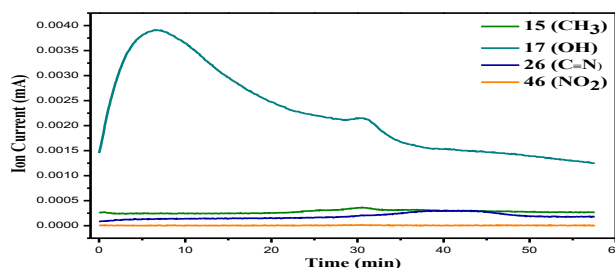


Figure 8. Mass spectrum of GA-ZnO-TiO<sub>2</sub> loaded with Entacapone

## 2.9. Invitro Drug Release Studies[8,9]

**Table 1.** Linearity data of GA-ZnO-TiO<sub>2</sub> - Entacapone

S. No.	Concentration ( $\mu\text{g/ml}$ )	Absorbance
1.	2	0.027
2.	4	0.041
3.	6	0.052
4.	8	0.068
5.	10	0.083
6.	12	0.098

**Table 1** illustrates the sequential absorbance values at different concentrations of the sample. A series of dilutions is done by taking the sample solution in potassium dihydrogen phosphate and ammonium hydroxide buffer solution. The test samples with concentrations 2, 4, 6, 8, 10, and 12  $\mu\text{g/ml}$  are prepared and the absorbance values for the corresponding concentrations are determined using a UV-visible spectrophotometer with  $\lambda_{\text{max}}$  305nm. It can be observed that the absorbance values increase upon increasing the concentration of the sample. Using these values, a standard graph or a calibration graph is plotted[25,26]

Linearity data of GA-ZnO-TiO<sub>2</sub> - Entacapone determines the standard curve or the calibration curve. The concentration values in  $\mu\text{g/ml}$  were graphed on the X-axis against the corresponding absorbance values on the Y-axis. The points lie on a straight line showing that the absorbance values increase with an increase in the concentration of the test sample[27].

### Percentage Drug Release Data

**Table 2.** Percentage drug release Data GA-ZnO-TiO<sub>2</sub> - Entacapone

S. No.	Time (min)	Absorbance	Corresponding Concentration ( $\mu\text{g/ml}$ )	Drug Release	%Drug release
1.	0	0.153	2.18	0.0109	10.9%
2.	5	0.194	2.77	0.0138	13.9%
3.	15	0.22	3.14	0.0157	15.7%
4.	30	0.31	4.42	0.0221	22.1%
5.	60	0.42	6.01	0.0300	30.0%
6.	120	0.58	8.28	0.0414	41.4%
7.	240	0.63	9.00	0.0450	45.0%
8.	480	0.74	10.57	0.0520	52.9%
9.	960	0.89	12.71	0.0630	63.0%
10.	1920	0.99	14.14	0.0700	70.7%

**Table 2** illustrates the percentage drug release values of the sample at different time intervals. Initially, a 100 $\mu\text{g/ml}$  concentration of the test sample is prepared, and the absorbance is determined using UV-visible Spectrophotometer at  $\lambda_{\text{max}}$  305nm. Similarly, the absorbance values for the same sample solution is determined at different time intervals. Using the drug release kinetics formula, the values of % Drug release is determined. From the table, it can be stated that the drug has extended release property and is slowly released with passage of time.

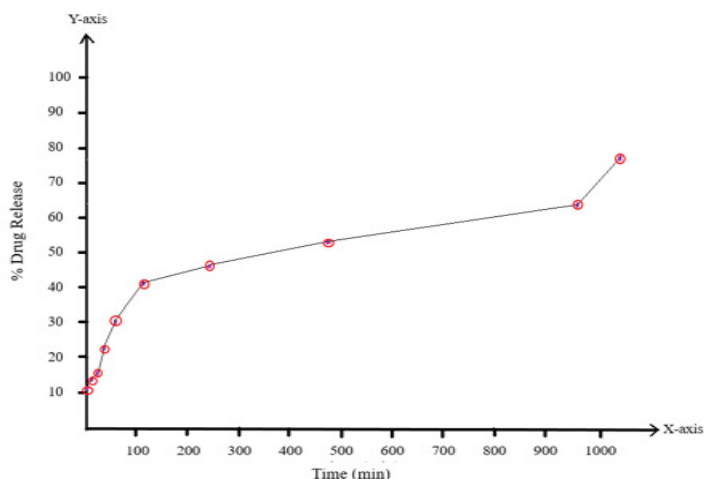


**Figure 9.** % Drug release graph of GA-ZnO-TiO<sub>2</sub>-Entacapone

Figure 9 depicts the percentage drug release of the sample at different time intervals. As time passes, there is an increase in the release of the drug substance showing an extended release or slow release of the drug. When the sample was initially prepared, the percentage of drug release was about 10.9%. With the increase in time, the drug release also increases and after 32 hours, i.e., 1920 minutes, the percentage of drug release was about 70.7%.

### 3. CONCLUSION

The present study describes the synthesis of Gum acacia-stabilized zinc oxide/titanium dioxide nanoparticles containing Entacapone, an antiparkinsonian drug. The co-precipitation method was employed for the preparation of these nanoparticles. Detailed characterization using various analytical techniques was conducted to assess their properties. Moreover, a thorough investigation into the release behavior of the drug revealed prolonged or sustained-release characteristics. By utilizing natural gum as a template and incorporating ZnO and TiO<sub>2</sub> as inorganic components along with entacapone, we achieved extended-release capabilities that enabled gradual release over time.

### 4. MATERIALS AND METHODS

#### 4.1. Materials

Entacapone an (Active pharmaceutical ingredient) was obtained from Sigma Aldrich (India). Gum acacia powder was obtained from AVRA labs(Hyderabad, India). Zinc acetate dihydrate from SD fine chemicals (Hyderabad, India) and Titanium isopropoxide were obtained from Sigma Aldrich (India) [28]. Deionized water was used as a solvent in the complete process of the GA-ZnO-TiO<sub>2</sub> nanocomposite synthesis process. All the other chemicals used in this process were of analytical grade.

#### 4.2. Synthesis of GA-ZnO-TiO<sub>2</sub> Nanoparticles

The aqueous solution of Gum acacia was prepared in 1%, 1.5%, and 2% w/v proportions. Add Zinc acetate dihydrate (1mmol) to the Gum acacia solution with continuous stirring for 15 mins. Similarly, add 1mmol of Titanium isopropoxide to the above mixture while stirring for 15 mins. The solution is then refluxed for 24 hours in an oil bath. 0.1M NaOH is added to the above precursor. The reflux was carried out for 5 more hours in an oil bath. The product was centrifuged and washed with ethanol and dried in an oven[29].

#### 4.3. Synthesis of Entacapone loaded GA-ZnO-TiO<sub>2</sub>

Entacapone (Active Pharmaceutical ingredient) was added to the aqueous solution of Gum acacia(1%) which was previously prepared by dissolving Gum acacia powder. The remaining process is similar to that of the GA-ZnO-TiO<sub>2</sub> nanoparticle. The product obtained is characterized for morphological, chemical, and thermal analysis[30,31].

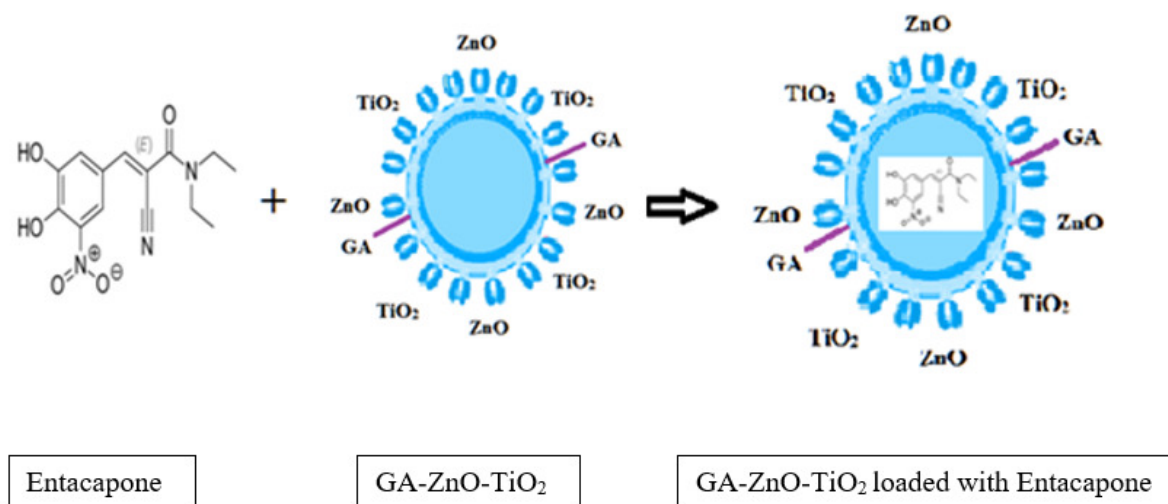


**Figure 10.** Schematic representation of GA-ZnO-TiO<sub>2</sub> nanoparticle synthesis

#### 4.4. Characterization

##### 4.4.1. X-ray diffraction (XRD)[32]

X-ray diffraction provides knowledge on phase identification, crystal size, morphology along sample purity. The research utilized the X-ray diffraction technique with Cu radiation, with the use of equipment from Rigaku in Tokyo, Japan. The Scherrer equation is employed for calculating the crystalline domain size (D) which is given as

$$D = \frac{K\lambda}{\beta \cos \theta}$$

##### 4.4.2. Scanning electron microscope (SEM):

Scanning electron microscopy (SEM) is a method/analysis process, widely used for high-resolution of 10.0K.eV imaging of surfaces that can be employed to characterize nanoscale materials. The synthesized nanoparticles' morphological characteristics and particle size assessment were studied using FFI Quanta 200 FEG with EDS scanning electron microscopy. The samples containing prepared Nanoparticles were diluted using distilled water and sonicated. A small drop of the sample was placed on a round cover glass (1.2cm) and allowed to dry in a desiccator at room temperature mounted on an SEM stub and coated with a thin layer of platinum to make the samples conductive for SEM analysis[33].

##### 4.4.3. Ultraviolet-Visible - Diffuse Reflectance Spectrum (UV-VIS-DRS):

UV-DRS assesses the composition of the compound depending upon spectral analysis of the reflected and fluorescent light upon exposure to the diffuse reflected light, measured using a Shimadzu UV 3600. Barium sulfate is used as a standard which has an absolute reflectance of 0.973-0.988. The samples were placed in the sample holder and scanned in a wavelength range of about 200-800nm. The reflectance spectra of the sample are recorded and plotted in 'Origin 7.0'[34].

##### 4.4.4. Differential scanning calorimetry (DSC):

The measurement of thermal transitions in a sample under inert atmosphere conditions is commonly carried out using thermal analysis techniques such as differential scanning calorimetry. The TA Instruments DSC-250 system model was employed in this study, coupled with an aluminum crucible as the sample holder.

To determine the enthalpies of the transitions, the heating rate was set to 100°C/min, and the temperature range examined was from 100°C to 2000°C. Nitrogen gas was used as the inert atmosphere during the experiment, and the runtime for each measurement was set to 20 minutes. The enthalpies of the transitions can be measured by using the following equation[35].

$$\Delta H = KA$$

#### 4.4.5. Thermogravimetry analysis (TGA):

To examine the thermal decomposition rate profile and assess the stability of a powdered sample, it is essential to employ thermogravimetric analytical techniques. This involves measuring mass changes over time by subjecting the sample to varying temperatures. For this particular study, we utilized a Thermo Gravimetric Analyser SDT Q 600 along with open aluminum crucibles as sample holders. The samples weighed approximately 6-8mg and were subjected to a heating rate of 10°C/min up until a temperature of 1000°C was reached. Throughout the experiment, nitrogen gas was employed to maintain an inert atmosphere. The overall duration of each run lasted for about 85 minutes[20,30,35].

#### 4.4.6. Derivative Thermal Gravimetry (DTG):

The variation in weight based on temperature and time can be investigated through Derivative Thermo Gravimetry. This technique involves heating the sample material which directly affects its weight change. The resulting changes in weight are recorded and used to create thermograms showing the relationship between weight and temperature. DTG experiments were conducted using a TA instrument with an aluminum holder for the samples weighing between 4-7mg at a heating rate of 10°C/min up to a temperature of 1000°C under a nitrogen atmosphere for 45 minutes[21,30,35].

#### 4.4.7. Fourier transform infrared spectroscopy (FTIR):

FTIR is a technique used to determine the chemical structure of numerous organic molecules, polymers, biological samples, inorganic compounds, minerals, semiconductors, etc. Infrared radiation correlates to the molecules' excitation energy, which is in the 1013–1014 Hz range. Model: Alpha-Bruker, Software: Opus-75 version, Window Material: Zinc-Selenium (Zn-Sc) ATR plates, Spectral Range: 4000 to 500 cm<sup>-1</sup>, Resolution: 16 scans [36].

#### 4.4.8. Mass Spectroscopy:

Mass spectroscopy is an analytical technique used to estimate the masses and reveal the chemical compositions of tiny nanoparticles. The elemental composition of the produced GA-ZnO-TiO<sub>2</sub> loaded with Entacapone nanoparticles was determined using mass spectroscopy, with the mass of the particles being determined by their charge ratios. By blasting the solid sample with electrons, a spectrum signal is produced, which is then detected by an electron multiplier. By comparing the masses of the detected masses in a distinctive fragmentation pattern with the masses of the elements present in the sample, the elements' presence may be determined by Thermo Scientific Exploris 120 mass spectrometry, Q-orbitrap analyzer, and APCI(Atmospheric pressure chemical ionization)[37].

#### 4.4.9. Release studies of the drug:

##### *Preparation of phosphate buffer*

Weigh sufficient quantities of potassium dihydrogen phosphate (KH<sub>2</sub>PO<sub>4</sub>) and sodium hydroxide (NaOH) and prepare a buffer solution using distilled water. The pH of this buffer solution was adjusted to 7.4[38].

##### *Preparation of the Test samples*

Test samples with concentrations 2, 4, 6, 8, 10, and 12 µg /ml were prepared using the above buffer solution. The absorbance of test samples was determined using a UV-visible spectrophotometer. A calibration graph is plotted[39,40].

**Acknowledgement:** I would like to thank DR. B. Sreedhar senior principal scientist, Analytical Department, CSIR, Hyderabad, India.

**Author contributions:** Concept – S.F., U.H.; Design – U.H., P.A., .; Supervision – S.F.; Resources – M.C., K.S.; Materials – S.A.; Data Collection and/or Processing – S.F., U.H.; Analysis and/or Interpretation – S.F., U.H., P.A., S.A.; Literature Search – K.S., M.C., P.A.; Writing – S.F.; Critical Reviews – S.F., U.H., P.A., M.C., K.S., S.A.

**Conflict of interest statement:** None

## REFERENCES

- [1] Iadnut A, Mamoon K, Thammasit P, Pawichai S, Tima S, Preechasuth K. In vitro antifungal and antivirulence activities of biologically synthesized ethanolic extract of propolis-loaded PLGA nanoparticles against candida albicans. *Evid Based Complement Altern Med.* 2019;3715481. <https://doi.org/10.1155/2019/3715481>
- [2] King, Stephen , Jarvie, Helen and Dobson, Peter. "nanoparticle". *Encyclopedia Britannica*, 8 Jan. 2024, <https://www.britannica.com/science/nanoparticle>. Accessed 18 July 2024.
- [3] Mahmoodzadeh H, Eshaghi A, Gholami T. Physiological analysis of CuO bulk and nanoparticles to castor (*Ricinus communis* L.). *Plant Breed.* 2016; 74(1): 45-56. <https://doi.org/10.1515/plass-2016-0014>
- [4] Patil US, Adireddy S, Jaiswal A, Mandava S, Lee BR, Chrisey DB. In vitro/in vivo toxicity evaluation and quantification of iron oxide nanoparticles. *Int J Mol Sci.* 2015; 16(10):24417-24450. <https://doi.org/10.3390/ijms161024417>
- [5] Hofmann C, Duerkop A, Baeumner A J. Nanocontainers for analytical applications. *Angew Chem Int Ed Engl.* 2019; 58(37): 12840-12860. <https://doi.org/10.1002/anie.201811821>
- [6] Jayachandran A, T R A, Nair AS. Green synthesis and characterization of zinc oxide nanoparticles using *Cayratia pedata* leaf extract. *Biochem Biophys Rep.* 2021; 8(26): 100995. <https://doi.org/10.1016/j.bbrep.2021.100995>
- [7] Smita N, Priyanka G, Bhaskar V. Green-synthesis of silver nanoparticles by *Hygrophila auriculata* extract: Innovative technique and comprehensive evaluation. *Indian J Pharm Educ Res.* 2021; 55(2s):s510-s517. <https://doi.org/10.5530/ijper.55.2s.122>
- [8] Padil V, Waclawek S, Černík M. Green synthesis: Nanoparticles and nanofibres based on tree gums for environmental applications. *Ecol Chem Eng S.* 2016;23(4): 533-557. <https://doi.org/10.1515/eces-2016-0038>
- [9] Rini AS, Rati Y, Fadillah R, Farma R, Umar L, Soerbakti Y. Improved photocatalytic activity of ZnO film prepared via green synthesis method using red watermelon rind extract. *Evergreen.* 2022; 9(4): 1046-1055. <http://dx.doi.org/10.5109/6625718>
- [10] Barik P, Bhattacharjee A, Roy M. Preparation, characterization and electrical study of gum arabic/ZnO nanocomposites. *Bull Mater Sci.* 2015; 38: 1609-1616. <https://doi.org/10.1007/s12034-015-0961-5>
- [11] Fabio F, Claudia F, Monica S, Mario S, Luisa D. *J Agric Food Chem.* 2018; 66 (26): 6860-6868. <https://doi.org/10.1021/acs.jafc.8b00747>
- [12] Vershney R, Chelaramani K, Bhardwaj A, Siddiqui M, Verma S. K. Synthesis photocatalytic and antibacterial activities of nickle doped tio<sub>2</sub> nanoparticles. *Orient J Chem.* 2018; 34(6): 3140-3144. <http://dx.doi.org/10.13005/ojc/340661>.
- [13] Gul N, Idrees QTA, Fareed MA, Mian SA, Nasim HMO, Naz F, Aldahlan B, Khan AS. Biological and physicochemical characterization of self-adhesive protective coating dental restorative material after incorporation of antibacterial nanoparticles. *Polym J.* 2022; 14(20):4280. <https://doi.org/10.3390/polym14204280>.
- [14] Hosseini, Seyed A, Shabnam B. Graphene Oxide/Zinc Oxide (GO/ZnO) nanocomposite as a superior photocatalyst for degradation of methylene blue (MB)-process modeling by response surface methodology (RSM). *J Braz Chem Soc.* 2016; 28: 299-307. <https://scite.ai/reports/10.5935/0103-5053.20160176>.
- [15] Ali K. Attia, Mona M. Abdel-Moety, Samar G. Abdel-Hamid. Thermal analysis study of antihypertensive drug doxazosin mesylate. *Arab J Chem.* 2017; 10: S334–S338. <https://doi.org/10.1016/j.arabjc.2012.08.006>.
- [16] Ashwini J, Aswathy TR, Rahul AB, Thara GM, Nair AS. Synthesis and characterization of zinc oxide nanoparticles using *Acacia caesia* bark extract and its photocatalytic and antimicrobial activities. *Catalysts.* 2021; 11(12):1507. <https://doi.org/10.3390/catal11121507>.
- [17] Talam S, Karumuri SR, Gunnam N. Synthesis, characterization, and spectroscopic properties of ZnO nanoparticles. *International Scholarly Research Notices.* 2012;2012(1):372505. <https://doi.org/10.5402/2012/372505>
- [18] Tang S, Liu Q, Hu J, Chen W, An F, Xu H, Song H, Wang YW. A simple colorimetric assay for sensitive Cu<sup>2+</sup> detection based on the glutathione-mediated etching of MnO<sub>2</sub> nanosheets. *Front Chem.* 2021; 9. <https://doi.org/10.3389/fchem.2021.812503>.
- [19] Gill P, Moghadam TT, Ranjbar B. Differential scanning calorimetry techniques: applications in biology and nanoscience. *J Biomol Tech.* 2010; 21(4): 167-193. <https://www.ncbi.nlm.nih.gov/pmc/articles/PMC2977967/>
- [20] Thomas R, Thomas S, Kumar R, Zachariah AK. Thermal and rheological measurement techniques for nanomaterials characterization. Elsevier Science & Technology Books.2017; 292 p.
- [21] Vyazovkin S, Schick C, Koga N. Handbook of Thermal Analysis and Calorimetry: Recent Advances, Techniques and Applications. Elsevier Science & Technology Books. 2018; 800 p.

- [22] Mirabella MF, editor. Modern techniques in applied molecular spectroscopy. New York: Wiley; 1998. 410 p.
- [23] Jain S, Jadav T, Sahu AK, Kalia K, Sengupta P. An exploration of advancement in analytical methodology for quantification of anticancer drugs in biomatrices. *Anal Sci.* 2019; 35(7):719-732. <https://doi.org/10.2116/analsci.19r002>.
- [24] Nishi KK, Antony M, Jayakrishnan A. Synthesis and evaluation of ampicillin - conjugated gum arabic microspheres for sustained release. *J Pharm Pharmacol.* 2007; 59(4): 485-493. <https://doi.org/10.1211/jpp.59.4.0002>.
- [25] Banerjee S, Chen DH. Glucose - grafted gum arabic modified magnetic nanoparticles: Preparation and specific interaction with concanavalin A. *Chem Mater.* 2007; 19(15): 3667-3672. <https://doi.org/10.1021/cm070461k>.
- [26] Mohan S, Vellakkat M, Aravind A, U R. Hydrothermal synthesis and characterization of Zinc Oxide nanoparticles of various shapes under different reaction conditions. *Nano Express.* 2020; 1(3): 030028. <https://doi.org/10.1088/2632-959x/abc813>.
- [27] Drug Bank - Entacapone, Educe Design & Innovation Inc. 2005; <https://go.drugbank.com/drugs/DB00494>.
- [28] Chockalingam A, Babu H, Chittor R, Tiwari J. Gum arabic modified Fe<sub>3</sub>O<sub>4</sub> nanoparticles cross linked with collagen for isolation of bacteria. *J Nanobiotechnol.* 2010; 8(1): 30. <https://doi.org/10.1186/1477-3155-8-30>
- [29] Wu CC, Chen DH. Spontaneous synthesis of gold nanoparticles on gum arabic-modified iron oxide nanoparticles as a magnetically recoverable nanocatalyst. *Nanoscale Res Lett.* 2012; 7(1): 317. <https://doi.org/10.1186/1556-276x-7-317>.
- [30] Thamer AA, Yusr HA, Jubier N J. TGA, DSC, DTG properties of epoxy polymer nanocomposites by adding hexagonal boron nitride nanoparticles. *J Eng Appl Sci.* 2019; 14(2): 567-574. <http://dx.doi.org/10.3923/jeasci.2019.567.574.7>.
- [31] Sreedhar B, Satya Vani C, Keerthi Devi D, V Basaveswara Rao M, Rambabu C. Shape controlled synthesis of barium carbonate microclusters and nanocrystallites using natural polysaccharide - Gum acacia. *Am J Mater Sci.* 2012; 2(1):5-13. <https://doi.org/10.5923/j.materials.20120201.02>.
- [32] Holder CF, Schaak RE. Tutorial on Powder X-ray Diffraction for characterizing nanoscale materials. *ACS Nano.* 2019; 13 (7): 7359-7365. <https://doi.org/10.1021/acsnano.9b05157>.
- [33] Srinivasan C, Mullen TJ, Hohman JN, Anderson ME, Dameron AA, Andrews AM, Dickey EC, Horn MW, Weiss PS. Scanning Electron Microscopy of Nanoscale Chemical Patterns. *ACS Nano.* 2007; 1(3): 191-201. <https://doi.org/10.1021/nm7000799>.
- [34] Syed A, Yadav LSR, Bahkali AH, Elgorban AM, Abdul Hakeem D, Ganganagappa N. Effect of CeO<sub>2</sub>-ZnO nanocomposite for photocatalytic and antibacterial activities. *Crystals.* 2020; 10(9):817. <https://doi.org/10.3390/cryst10090817>.
- [35] Perez-Nakai A, Lerma-Canto A, Dominguez-Candela I, Garcia-Garcia D, Ferri JM, Fombuena V. Comparative study of the properties of plasticized polylactic acid with maleinized hemp seed oil and a novel maleinized Brazil nut seed oil. *Polymers.* 2021; 13(14): 2376. <https://doi.org/10.3390/polym13142376>.
- [36] Wilson AC, Chou SF, Lozano R, Chen JY, Neuenschwander PF. Thermal and physico-mechanical characterizations of thromboresistant polyurethane films. *Bioeng.* 2019; 6(3): 69. <https://doi.org/10.3390/bioengineering6030069>.
- [37] Vergara S, Santiago U, Kumara C, Alducin D, Whetten RL, Jose Yacaman M, Dass A, Ponce A. Synthesis, mass spectrometry, and atomic structural analysis of Au~2000(SR)~290 nanoparticles. *J Phys Chem C.* 2018; 122 (46): 26733-26738. <https://doi.org/10.1021/acs.jpcc.8b08531>.
- [38] Syed A, Yadav LS, Bahkali AH, Elgorban AM, Abdul Hakeem D, Ganganagappa N. Effect of CeO<sub>2</sub>-ZnO nanocomposite for photocatalytic and antibacterial activities. *Crystals.* 2020; 10(9):817. <https://doi.org/10.3390/cryst10090817>.
- [39] Devi S, Kumar S, Verma V, Kaushik D, Verma R, Bhatia M. Enhancement of ketoprofen dissolution rate by the liquisolid technique: optimization and in vitro and in vivo investigations. *Drug Deliv Transl Res.* 2022; 12(11): 2693-2707. <https://doi.org/10.1007/s13346-022-01120-x>.
- [40] Kumar G, Patrudu TB, Rao TN, Rao MV. A new analytical method validation and quantification of entacapone and its related substance in bulk drug product by HPLC. *Asian J Pharm Ana.* 2017; 7(1): 1-5. <https://doi.org/10.5958/2231-5675.2017.00001.1>